TSF002

Feasibility study of flameless combustion in a can-type swirl combustor without a modification

Seekharin Komonhirun*, Pisit Yongyingsakthavorn and Udomkiat Nontakeaw

Department of Mechanical and Aerospace Engineering,
King Mongkut's University of Technology North Bangkok, Bangkok, Thailand
*Corresponding author: k.seekharin@gmail.com

Abstract

Previous work is preliminary design of a lean-combustion can-type swirl combustor for the 30-KW micro gas turbine using the biogas as fuel; it is found that NO_x emission is still high at 25 ppm/hr. Flameless combustion is one effective method, where NO_x formation can be suppressed to a zero level (1.175x10^{-15}ppm/hr). In this research, the flameless combustion is studied and applied to the designed can-type swirl combustor. NO_x concentration is observed through a numerical method by FLUENT. The selected turbulent and combustion models are RNG k-ε and non-premixed, respectively, and compressibility effects are also accounted. The results show that the combustion temperature is drastically dropped. The NO_x concentration of both prompt NO_x and thermal NO_x could be reduced and approaches to the zero value (7.52x10^{-7} ppm/hr). This results show that there is the feasibility to applying the complete flameless combustion on any typical swirl combustors without their modification in order to reduce NO_x concentration to the zero level.

***Keywords**:* flameless combustion, can-type combustor, NO_x reduction, FLUENT

1. Introduction

Combustion and its emissions control are essential as far as the most of energy use is from combustion sources. The major emissions are unburned and partial burned hydrocarbons, nitrogen oxides (NO and NO2), carbon monoxide, sulfur oxides (SO and SO2), and particulate matter [1]. In the United State, pollution problem is critical in the middle of the 20th century. Many researches have been done to reduce the emissions that were being increased. Many emissions were able to be reduced except NOx. Thus, there are many works to study mechanisms of NOx formation later. As the work done by Gao et al. [2], Both experimental and numerical studies of NO_x reaction mechanism are carried out and found that there are 4 interested types of NO_x reaction pathways, which generates NO_x concentration inside the combustor. Prompt NO_x and NNH reactions which are normally activated in reaction zone, a narrow gap between a high and low fuel concentration zone, thermal NO_x in any high temperature environment and N_2O are NO_x which caused by a reaction of other radicals. They concluded that if the peak temperature is depleted and the overall temperature of combustion is reduced, then all of the NO_x pathways are suppressed.

Nevertheless, the green technology and the zero emission combustion have currently been being more and more recognized as pollution and global warming problems still be extended. One effective method is a flameless combustion that can drastically reduce emissions. A flameless combustor is a NO_x prevention method that suppressed NO_x reaction pathways, because the NO_x reactions have insufficient activation energy. In fact, the flameless combustion was accidentally discovered in 1989 by Wunning [3]. He found a strange phenomenon in a self-recuperative furnace. This phenomenon occurs only when the temperature of a self-recuperative furnace reaches approximately 1,000 ^{O}C and the inlet air temperature is above the auto-ignition temperature of fuels. It appears that the flame suddenly vanishes, and cannot be detected in both UV and visible light wavelengths, but it glows only in infrared wavelengths. The combustion in this mode is smooth and stable while the amount of NO_x is reduced to near zero value. This combustion phenomenon is thus called a Flameless oxidation reaction or FLOX®.

Abuelnuor et al. [4] describe the flameless oxidation reaction (FLOX®) mechanism that it needs two requirements. First, the inlet air must be preheated until its temperature is above an auto-ignition temperature of fuels which air-fuel mixture is suddenly combusted. Second, the internal recirculation flow by exhaust gas would reduce an oxygen concentration, which suppresses the peak temperature and distributes combustion smoothly in an entire combustion chamber and increase a combustion efficiency as demonstrate in Fig 1.

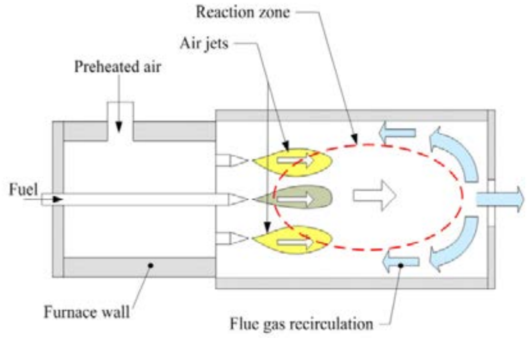

Fig.1 Flameless combustion mechanism

Hosseini et al. [5] have numerically studied both preheated and flameless combustion of methane and biogas fuels. It is shown that NO_x is very low for biogas because of its less fuel concentration when compared to methane. Lower fuel concentration leads to reduction of combustion temperature. NO_x is increased in preheated combustion, especially in the case of methane. In flameless combustion, NO_x can be reduced by controlling combustion rather uniform inside the combustor to discard the peak temperature that causes NO_x. This result agrees to the work done by Gao et al. They also observed the effects of oxidizer percentage of inlet air by varying from 5% to 15%. This is one approach apart from exhaust gas recirculation to reduce oxygen concentration for flameless combustion mode. They discovered that the less the oxidizer percentage, the more the flameless combustion effective is. The combustion flame is rapidly diluted by N_2 or any inert gas, which is the important condition for the flameless combustion. By the works reviewed above, it ensures that the flameless combustion is the effective method for NO_x reduction.

According to the former research, preliminary design of a lean combustion can-type combustor for a 30-KW micro gas turbine has been carried out [1]. The combustion stability was numerically studied. The effects of the swirl number and combustion chamber aspect ratios were investigated. The equivalent ratio (ϕ = 0.6) and Reynolds number (Re_{air}/Re_{fuel} = 0.42) was maintained constant. It was found that the combustor size and the swirler angle are important parameters that control the combustion stability. The swirler angle controls stability through reverse flow of a fuel jet promoting air-fuel mixing effectiveness and combustion efficiency. Nevertheless, the emission is still released.

In this research, the feasibility of NOx reduction by flameless combustion on the available can-type swirl combustor without any modification is studied. NO_x concentration is investigated through numerical approach.

2. Governing Equations

Governing Equations employed in this work include:

Continuity equation:

$$\frac{\partial \rho}{\partial t} + \nabla(\rho\vec{v}) = 0 \tag{1}$$

RNG k-ε turbulent model which consists turbulent kinetic equation (k-equation):

$$\frac{\partial}{\partial t}(\rho k) + \frac{\partial}{\partial x_i}(\rho k u_i) = \frac{\partial}{\partial x_j}\left(\alpha_k \mu_{eff}\frac{\partial k}{\partial x_j}\right)$$
$$+G_b + G_k - \rho\epsilon - Y_M \tag{2}$$

and turbulent dissipation equation (ε-equation):

$$\frac{\partial}{\partial t}(\rho\varepsilon) + \frac{\partial}{\partial x_i}(\rho\varepsilon u_i) = \frac{\partial}{\partial x_j}\left(\alpha_k \mu_{eff}\frac{\partial \varepsilon}{\partial x_j}\right)$$
$$+C_{1\varepsilon}\frac{\varepsilon}{k}(G_k + C_{3\varepsilon}G_b) - C_{2\varepsilon}\rho\frac{\varepsilon^2}{k} - R_\varepsilon \tag{3}$$

Ideal gas equation for compressible condition is given by

$$P = \rho RT \tag{4}$$

The flameless combustion is considered to be non-premixed combustion, which has been applied to the design swirl can-type combustor, similar to the previous work. An energy equation for non-premixed combustion in terms of total enthalpy (H) of all species then is:

$$\frac{\partial}{\partial t}(\rho H) + \nabla\cdot(\rho\vec{v}H) = \nabla\cdot\left(\frac{k_t}{c_p}\nabla H\right) \tag{5}$$

The two main equations concerning mixture fraction transport and mixture fraction variance are, respectively, given by:

$$\frac{\partial}{\partial t}(\rho\bar{f}) + \nabla\cdot(\rho\vec{v}\bar{f}) = \nabla\cdot\left(\frac{k_t}{c_p}\nabla\bar{f}\right) \tag{6}$$

$$\frac{\partial}{\partial t}(\rho\overline{f'^2}) + \nabla\cdot(\rho\vec{v}\overline{f'^2}) = \nabla\cdot\left(\frac{\mu_t}{\sigma_t}\nabla\overline{f'^2}\right)$$
$$+C_g\mu_t(\nabla\bar{f})^2 - C_d\rho\frac{\varepsilon}{k}\overline{f'^2} \tag{7}$$

For NO_x transport and species transport which describe by mass fraction of species (Y_i), the equations are:

$$\frac{\partial}{\partial t}(\rho Y_{NO}) + \nabla\cdot(\rho\vec{v}Y_{NO}) = \nabla\cdot(\rho D\nabla Y_{NO}) + S_{NO} \tag{8}$$

and

$$\frac{\partial}{\partial t}(\rho Y_i) + \nabla\cdot(\rho\vec{v}Y_i) = \nabla\cdot(\rho D\nabla Y_i) + S_i \tag{9}$$

respectively.

3. Numerical Simulation

In general, injections of air supply are different between a swirl combustor and a typical flameless combustor. This would lead to different flow pattern and also combustion characteristics inside the combustion chamber. First of all, the flameless combustion is studied by using the combustor from the other work (Hosseini et al. [5]) in order to repeat their work and ensure that the same result is obtained. After that, the baseline swirl can-type combustor designed in the previous work is studied for feasibility of NOx reduction by flameless combustion. The effects of different of flow patterns on occurrence of flameless combustion will be investigated.

3.1 Model Geometries

The flameless combustor from the work done by Hosseini et al [5]. is illustrated in Fig. 2. It is clearly seen that the injection of air combustion is different from that of the baseline swirl can-type combustor as shown in Fig. 3. The fuel inlet diameter of the baseline combustor is 5 mm. Fig. 4 shows the air swirler.

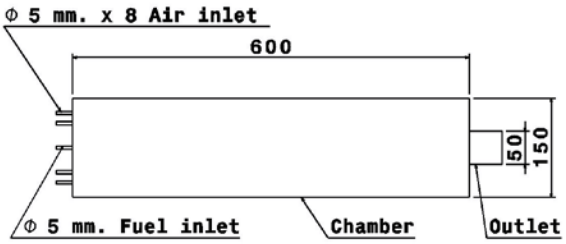

Fig. 2 Flameless combustor model

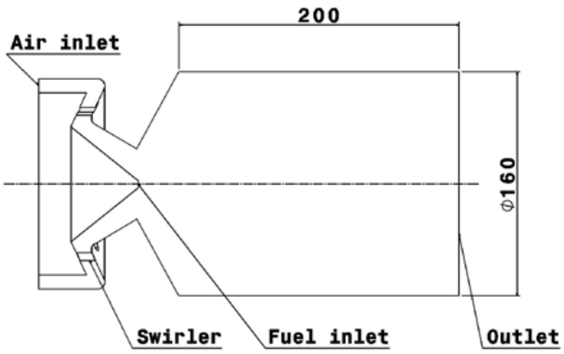

Fig. 3 The baseline can-type combustor

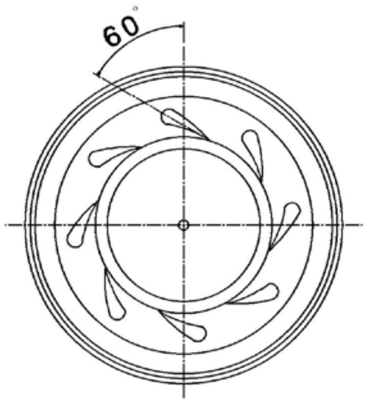

Fig. 4 The swirler of the can-type combustor

3.2 Boundary Conditions

There are four cases studied in this work. Case 1 is the conditions applied on the flameless combustor from the other work while Case 2-4 are the conditions applied on our designed combustor. Table 1 presents the boundary conditions of the case 1. The fuel utilized is biogas and the equivalent ratio is equal to 1. The oxidizer compositions are N_2 of 95% and O_2 of 5%. Its temperature is at 627 ^OC and the pressure equals 1 atm. In this case, the result consistent with Hosseini's work [5] is expected.

Table 1 The flameless boundary conditions (Case 1)

Boundary Conditions	Value
Biogas Composition	CH_4 60% , CO_2 40%
Oxidizer Composition	N_2 95% ,O_2 5%
Inlet Air Temperature	900K (627 ^OC)
Inlet Fuel Temperature	300K (27^OC)
Equivalent ratio ϕ	1
Pressure	1 atm

Next, the available can-type swirl combustor without any modification from the previous is studied. For Case 2, the boundary conditions are the operating conditions for the micro gas turbine where the pure methane is used as the fuel (see Table 2). The combustion is lean, which ϕ is equal to 0.6. The oxidizer compositions are N_2 of 73% and O_2 of 21%. The preheated air temperature is 510 ^OC and the pressure is high at 3.5 bars. In Case 3, the oxidizer compositions and its temperature are changed to be same with case 1 (N_2 = 73%, O_2 = 21% and 627 ^OC). In Case 4, the available can-type swirl combustor is finally applied with the conditions like in Case 1 except the pressure is still higher at 3.5 bars.

Table 2 Preheated swirl lean combustion boundary conditions (Case 2)

Boundary Condition	Value
Pure methane	CH_4 100%
Oxidizer Composition	N_2 73% ,O_2 21%
Inlet Air Temperature	783K (510 ^OC)
Inlet Fuel Temperature	300K (27^OC)
Equivalent ratio ϕ	0.6
Pressure	3.5 bar

Table 3 The flameless swirl lean combustion boundary conditions with pure methane (Case 3)

Boundary Conditions	Value
Pure methane	CH_4 100%
Oxidizer Composition	N_2 95% ,O_2 5%
Inlet Air Temperature	900K (627 ^OC)
Inlet Fuel Temperature	300K (27^OC)
Equivalent ratio ϕ	0.6
Pressure	3.5 bar

Table 4 The flameless swirl lean combustion boundary conditions with biogas (Case 4)

Boundary Conditions	Value
Biogas Composition	CH_4 60% , CO_2 40%
Oxidizer Composition	N_2 95% ,O_2 5%
Inlet Air Temperature	900K (627 ^OC)
Inlet Fuel Temperature	300K (27^OC)
Equivalent ratio ϕ	0.6
Pressure	3.5 bar

3.3 Numerical Procedure

In this research, the Ansys Fluent 14 is responsibly applied to the problems by using a 3D finite volume analysis. The tetrahedral meshes are generated for all cases. The simulation results from the four combustion conditions are analyzed and compared. The CFD numerical procedures solving by the RANS equations and species transport equations described in section 2 are employed. A steady flow pressure-base solver is applied with added up compressible effects, high swirl flow for swirl combustion, and inlet fuel diffusion. All numerical schemes are a secondary upwind method. For convergent absolute criteria, iterations and residuals are set equal to 50,000 and 10^{-6}, respectively. In the next section, the simulation results for different cases are presented and discussed, including thermal and prompt NO_x concentration, temperature and velocity.

4. Simulation Results and Analysis

From the simulation results, it is found that temperature appears to be smoothly distributed along the original flameless combustor (see Fig. 5). There are no significant high temperature spot in wide space. It is limited within a very narrow volume near downstream of each fuel (biogas) injector. The highest spot is less than 1,300 K. The temperature is widely spread at the level around 1,000 K (800 ^{O}C). Streamline in Fig. 6 shows the four vortexes near the air inlet, which is due to the jet stream recirculation. These vertexes results in re-burning exhaust gases before releasing at outlet.

This flameless phenomenon can occur by two conditions, which are the high oxidizer temperature above an auto-ignition point and oxygen dilution (O_2 is diluted at 5% for Case 1). The first condition causes rapid combustion while the second condition promotes energy absorption by carbon-dioxide and inert gas leading to disappearance of flame and drastic drop of temperature. These are the reasons why NO_x reaction cannot activate in this circumstance.

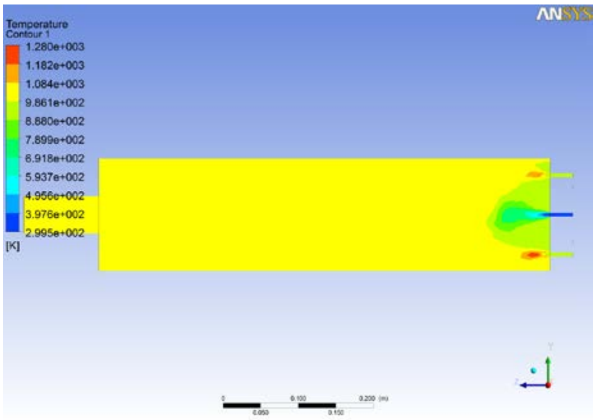

Fig. 5 Temperature of the flameless combustor in Case 1

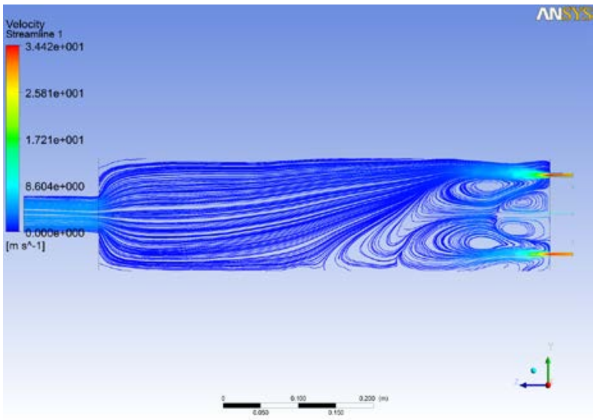

Fig. 6 Streamline of the flameless combustor in Case 1

In the swirl can-type combustor, its air injection differs from that of the original flameless combustor. Instead of the simple direct air injection, the air is injected through a swirler inducing the swirl flow, which promoting air-methane mixing in the combustion chamber. This difference is a challenge to have flameless combustion mode in the typical swirl can-type combustor without any modification.

Figures 7 and 8 demonstrate the results of temperature and streamline of the baseline swirl can-type combustor in Case 2. The temperature distribution shows the peak temperature around 2,500 K (2,227^{O}C). This result indicates that the combustion temperature is still high and NOx mechanism is well activated as explained by Gao et al. [2].

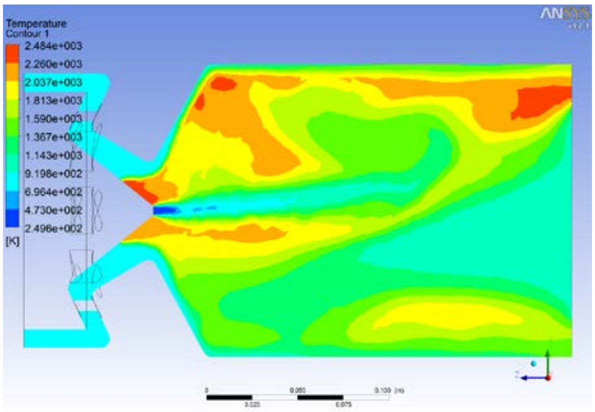

Fig. 7 Temperature of the swirl combustor in Case 2

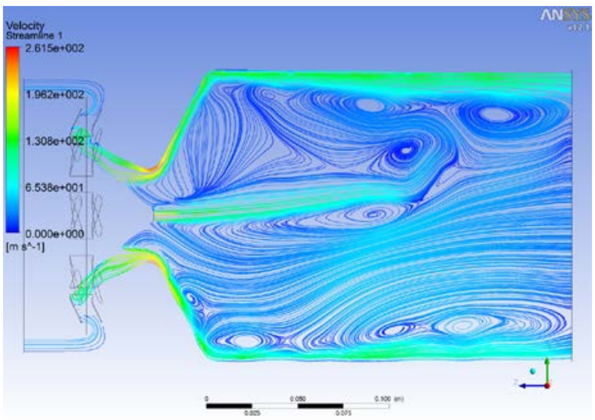

Fig. 8 Streamline of the swirl combustor in Case 2

After applying flameless conditions in Case 3, the peak temperature is drastically dropped in combustion zone and temperature diffusion area is wider as shown in Fig. 9. The peak temperature is 1,474 K (1,201^{O}C) which is 1,026 K lower than that in Case 2. At the same time, the streamline pattern appears different from Case 2. The vortexes formed are not to be disordered like in Case 2 and the resident time tends to be increased. Combustion stability in the swirl combustor seems to be not affected by the flameless conditions. On the other hand, decrease of the peak temperature would reduce the production rate of NO_x.

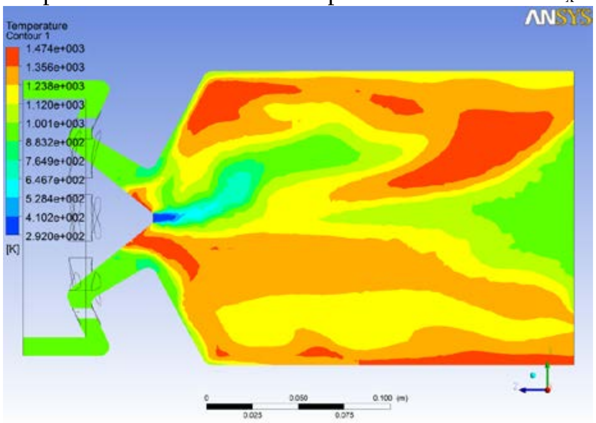

Fig. 9 Temperature of the swirl combustor in Case 3

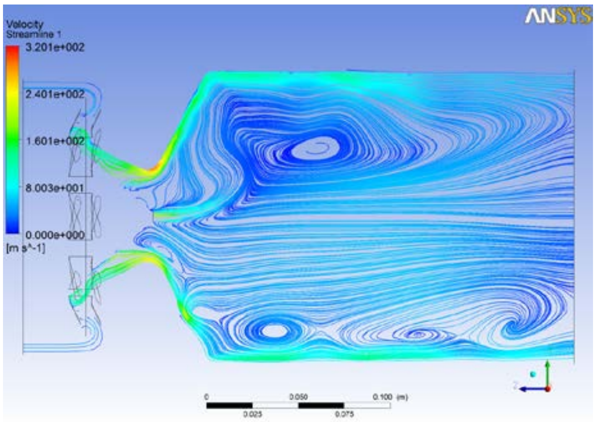

Fig. 10 Streamline of the swirl combustor in Case 3

Figures 11 and 12 show the temperature distribution and streamline in Case 4. The fuel is replaced from pure methane to biogas in which the mixture is more diluted by CO_2 in the fuel. The results show that a peak temperature is slightly decrease compare to Case 3. This is due to the fact that an adiabatic temperature of the biogas is lower than that of the methane. This means that using biogas as the fuel promotes flameless combustion and NO_x prevention rather than using the methane. Streamline pattern is slightly change from Case 3; it tends to be more symmetrical with the large coupling vortexes.

Fig. 13 presents the rates of thermal and prompt NO_x concentration for all cases. It is seen that NO_x concentration is lowest in Case 1 and largest in Case 2. NOx production rate is reduced from Case 2 to Case 4 when the hot spot is limited in narrower space and the peak temperature is lower, in which the combustion approaches to the flameless situation. Notice that, the production rate of prompt NO_x is lower than the thermal NO_x for all cases of the swirl combustor but it is opposite in the case of the flameless combustor, in which the prompt NOx slightly higher than thermal NOx.

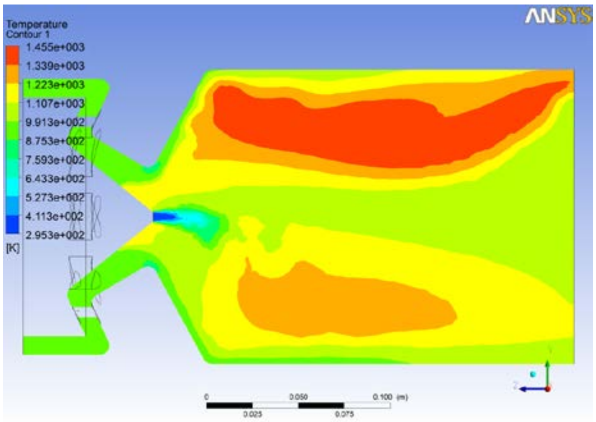

Fig. 11 Temperature of the swirl combustor in Case 4

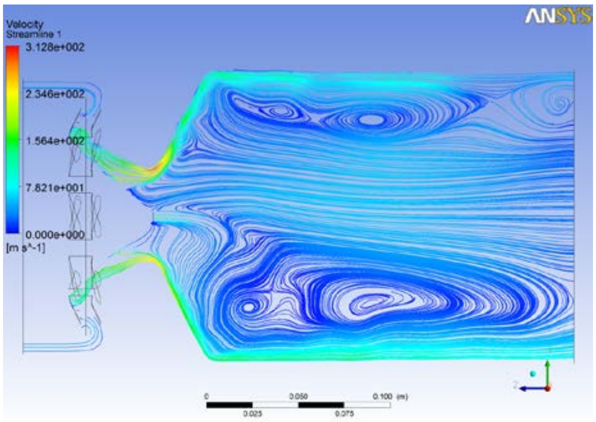

Fig. 12 Streamline of the swirl combustor in Case 4

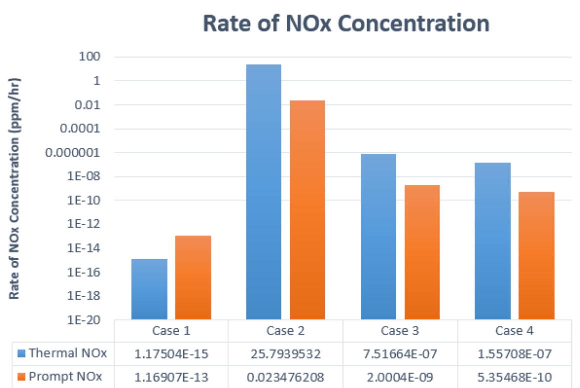

Fig. 13 Comparison of rates of NO_x concentration in logarithm scales

From all above results, it is no doubt that NO_x elimination is successful by applying the flameless condition on the available swirl can-type combustor without any geometrical modification, even though the complete flameless phenomena seem not to be achieved yet. Furthermore, it also seems that there is the feasibility to apply flameless combustion on any typical swirl combustors, in order to reduce NOx to the zero level.

5. Conclusion

The feasibility of using the can-type swirl combustor in flameless mode without any modification is studied. There are four study cases to compare. Case 1 is the study of the flameless biogas combustion on an original flameless combustor. Cases 2 to 4 are the study of combustion with different conditions on the available swirl can-type combustor from the previous work. Case 2 is the air-preheated swirl lean combustion by using methane as fuel. Case 3 is the flameless swirl lean combustion with the same fuel. In Case 4, the combustion conditions are the same to Case3 except the fuel is replaced by biogas.

The results show that the original combustor (Case 1) yields the smallest rate of NOx (thermal and prompt). For swirl can-type combustor (Cases 2-3), the peak temperature is drastically decreased when the flameless condition is applied leading to effective NOx reduction. Furthermore, using the biogas as the fuel also promote flameless combustion and NOx reduction (Case 4). Although, this NOx rate is still higher than that found in the flameless combustor as Case 1, it shows good feasibility to achieve the complete flameless application in any typical swirl can-type combustors without a geometrical modification. These results should be validated by an experimental work, which is expected to be performed in the next step.

6. Acknowledgement

The authors would like to thank to the "Development of Machinery and Industrial Equipment (DMIE)" research center, and to Mechanical and Aerospace Engineering (MAE) Department of the King Mongkut's University of Technology North Bangkok (KMUTNB) for supporting the numerical software "FLUENT" and other facilities.

7. References

[1] S. Komonhirun, P. Yongyingsakthavorn and U. Nontakeaw, "Preliminary Design of the Lean-Combustion Can-type Combustor for the 30-kW Micro gas turbine" TSME-ICoME 2013, AEC-1019

[2] X. Gao, F. Duan, S. C. Lim, and M. S. Yip, "NO_x formation in hydrogen–methane turbulent diffusion flame under the moderate or intense low-oxygen dilution conditions," Energy, vol. 59, pp. 559–569, Sep. 2013.

[3] J. G. Wünning, "FLAMELESS COMBUSTION AND ITS APPLICATIONS," pp. 1–12.

[4] A. A. A. Abuelnuor, M. a. Wahid, S. E. Hosseini, a. Saat, K. M. Saqr, H. H. Sait, and M. Osman, "Characteristics of biomass in flameless combustion: A review," Renew. Sustain. Energy Rev., vol. 33, pp. 363–370, May 2014.

[5] S. E. Hosseini, G. Bagheri, and M. A. Wahid, "Numerical investigation of biogas flameless combustion," Energy Convers. Manag., vol. 81, pp. 41–50, May 2014.